Tutorial 8: Discovery of the Higgs boson

Dr. M Flowerdew

May 6, 2014

1 Introduction

From its inception in the 1960's, the Standard Model was quickly established, but it took about 50 years for all of the predicted particles to be discovered. The last to be found was the elusive Higgs boson, the discovery of which was announced[1] by the ATLAS and CMS collaborations on July 4th 2012.

You will recall from tutorials 2 and 3 that the Higgs boson arises as a consequence of giving mass to the other SM particles, while retaining $\text{SU}(3) \times \text{SU}(2) \times \text{U}(1)$ gauge symmetry in the Lagrangian. This mechanism (called the *Brout-Englert-Higgs* or BEH mechanism), was the cause of the subsequent Nobel Prize awarded to Englert and Higgs in 2013. As three of the four components of the Higgs field are "eaten" by the W and Z gauge bosons, the Higgs boson is the only direct evidence for the existence of this mechanism. All of the interactions of this boson are fixed by existing SM measurements, the only unknown parameter is the boson's mass m_h, as discussed in tutorial 6.

Before discussing the discovery of the Higgs boson, it is important to understand its production and decay mechanisms in high energy pp collisions. This is discussed in the next section.

2 Production and decay of the Higgs boson at the LHC

The Lagrangian interaction terms relevant for the current discussion are the following:

$$\mathcal{L}_{h \text{ int}} = \frac{2m_W^2}{v} W_\mu^- W^{+\mu} h + \frac{m_Z^2}{v} Z_\mu Z^\mu h \tag{1a}$$

$$- \left[\frac{m_e}{v} \bar{\ell}_{\text{L}} e_{\text{R}} h + \frac{m_d}{v} \bar{q}_{\text{L}} d_{\text{R}} h + \frac{m_u}{v} \left(-\bar{d}_{\text{L}} \quad \bar{u}_{\text{L}} \right) u_{\text{R}} h + \text{h.c.} \right]. \tag{1b}$$

These describe vertices between the Higgs boson and two other SM particles. Interactions between three and four Higgs bosons have not been included,

---

[1] Initially, as a "Higgs-like particle".

(a) Decay to fermions   (b) Decay to W and Z bosons   (c) Decay to photons
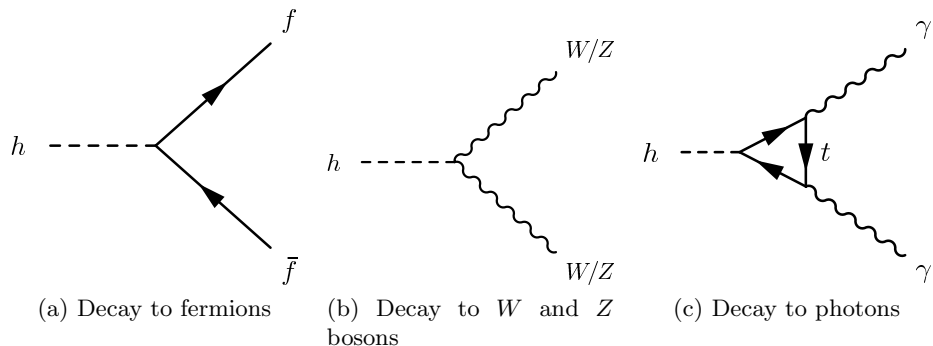
Figure 1: Decay modes of the Higgs boson.

nor have the quartic interactions between two Higgs bosons and two gauge bosons[2].

Exercise: Derive Equation (1), using the full SM Lagrangian given in tutorial 3. You may assume that $Y_e = m_e$ etc. *Hint:* The boson part is already partly developed in Equation (12) from tutorial 3.

From Equation (1), it can be seen that the Higgs boson couples to each other SM particle with a strength that depends on the particle's mass (remember that for fermions this is described by a Yukawa coupling not predicted by the theory). This fact has a profound effect on the phenomenology of the Higgs boson, meaning that it predominantly couples to the top quark and the W and Z bosons, and more weakly to the bottom quark and tau lepton. The direct coupling of the Higgs boson to other SM particles can be neglected for most practical purposes.

2.1 Higgs boson decay modes

We begin this discussion of Higgs phenomenology by considering how a real (i.e. on-shell) Higgs boson will decay once produced. Diagrams for the principal decay modes are shown in Figure 1. In subfigures (a) and (b), the Higgs boson decays directly into two massive particles, via a three-particle vertex described by the Lagrangian terms above. The branching ratios for different decay modes are shown in Figure 2, as a function of the Higgs boson mass. It can be seen that, for $m_h \lesssim 135$ GeV, the decay $h \to b\bar{b}$ is dominant. This is simply because the b quark is the most massive particle that is kinematically accessible for a Higgs boson within that mass range. The decays into other fermion-antifermion pairs ($\tau^+\tau^-$, $c\bar{c}$, $\mu^+\mu^-$ etc) are heavily suppressed with respect to the $b\bar{b}$ mode, due to the relatively small masses of these particles. At even higher masses ($m_h \gtrsim 400$ GeV), the decay

---

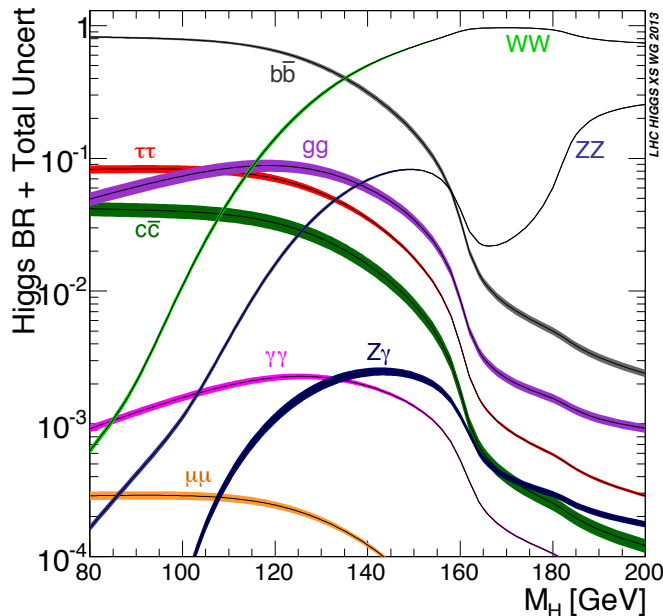[2]Why are these not relevant for (single) Higgs boson production and decay at the LHC?

Figure 2: Branching ratios for different Higgs boson decay modes, as a function of the boson's mass.

to top quarks becomes possible, although it never achieves more than a 20% branching ratio, due to kinematic and other factors.

As the Higgs boson mass increases, the decay channels $h \rightarrow W^+W^-$ and $h \rightarrow ZZ$ become kinematically accessible[3]. These become the dominant Higgs boson decay modes for large m_h, with the WW mode in particular approaching 100% of all decays for $160 \lesssim m_h \lesssim 175$ GeV. The Z boson has a slightly larger mass than the W, but a comparison of the relevant terms in Equation (1) makes it clear that there is a relative factor of 2 between the ZZh and WWh couplings, even once the difference between m_Z and m_W has been taken into account. Thus, the WW decay mode continues to dominate even when $m_h >> 2m_Z$.

The three remaining decay modes in Figure 2 are $h \rightarrow \gamma\gamma$, $h \rightarrow gg$ and $h \rightarrow Z\gamma$. Of these, the diphoton decay mode is by far the most important experimentally. All three modes are impossible at tree level, as the gluon and photon are both massless particles and do not couple directly to the Higgs field. Instead, they proceed via loop diagrams, such as the one shown in Figure 1 (c). In principle, all fermions and bosons with appropriate

---

[3]It should be noted that, below 161 GeV and 182 GeV, respectively, these are three-body decays that proceed via one off-shell boson, e.g. $h \rightarrow ZZ^* \rightarrow Zf\bar{f}$. However, as modern calculations correctly take off-shell contributions into account (including when both bosons are off-shell), there is no need to artificially introduce discontinuities at these masses.

charges can contribute to the loop, but the top quark provides the largest contribution, due to its large coupling to the Higgs boson.

In summary, a Standard Model Higgs boson with $m_h = 125$ GeV decays with the following branching ratios, as calculated by the LHC Higgs cross-section working group[4]:

Decay channel	Branching ratio
$h \to b\bar{b}$	58%
$h \to W^+W-$	22%
$h \to gg$	8.6%
$h \to \tau^+\tau^-$	6.3%
$h \to c\bar{c}$	2.9%
$h \to ZZ$	2.6%
$h \to \gamma\gamma$	0.2%

Many of these channels are difficult, if not impossible, to detect against the overwhelming background from QCD interactions at the LHC. This especially applies when the Higgs boson decays only into jets, including the dominant decay channel, $b\bar{b}$. The most sensitive channels in general are those where the Higgs boson decays into photons or leptons. However, these channels have very small branching ratios. The $\tau\tau$ channel has a relatively high branching ratio of over 6%, but this is offset by the low identification efficiency for hadronic τ lepton decays, and the diphoton branching ratio is 0.2%. Taking contributions from both $h \to W^+W^-$ and $h \to ZZ$ into account, the branching ratio $h \to \ell^+\ell^-\nu\bar{\nu}$ is 1.1%, while the four-lepton channel $h \to \ell^+\ell^-\ell^+\ell^-$ has a branching ratio of just 1.3×10^{-4}. These small branching ratios require large amounts of data to be collected before the Higgs boson can be detected. To understand this, we need to see how a Higgs boson might be produced in pp collisions.

2.2   Higgs boson production modes

There are four main production mechanisms for a Higgs boson at the LHC; these are illustrated in Figure 3. The cross-sections for these processes are shown in Figure 4, as a function of m_h. The dominant production method is called *gluon fusion* (Figure 3 (a)), and proceeds through a top quark loop, as the gluon itself is massless. This process has the largest cross-section despite the loop, due to the large top Yukawa coupling and the large value of the parton density function for gluons at the LHC (see tutorial 5, especially Figure 4 (c)). The cross-section for this process, assuming $m_h = 125$ GeV and $\sqrt{s} = 8$ TeV, is about 20 pb, meaning that in 20 fb^{-1} of pp collisions collected by each of ATLAS and CMS in 2012, approximately 400,000 Higgs bosons have been produced. However, the identification of the Higgs bosons

---

[4]Note that the numbers do not add to 100% due to rounding, and that some minor modes have been omitted.

(a) Gluon fusion (b) Vector boson fusion

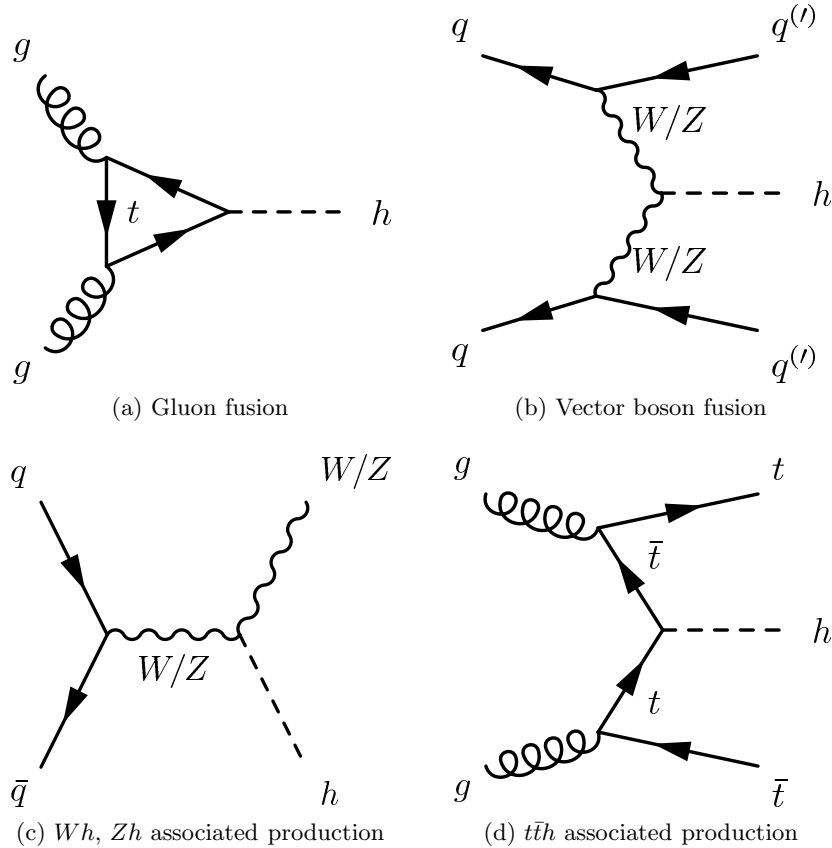(c) Wh, Zh associated production (d) $t\bar{t}h$ associated production

Figure 3: Production mechanisms for the Higgs boson in proton-proton collisions.

that decay only to jets is impossible at the LHC, leaving only the very small fraction that decay into photons or leptons available for study.

The next most common production mechanism is *vector boson fusion* (VBF, Figure 3 (b)). This is suppressed with respect to gluon fusion by the smaller quark pdfs and the electroweak vertices needed to produce the gauge bosons, but the two jets produced in additional to the Higgs boson have particular properties that help to separate VBF Higgs production from background processes in a way that is impossible for gluon fusion. The cross-section for this process in pp collisions with $\sqrt{s} = 8$ TeV is approximately 1.6 pb if $m_h = 125$ GeV.

Figures 3 (c) and (d) show the *associated production* modes of the Higgs boson. These are supressed with respect to the other production modes by the requirement to produce massive particles in addition to the Higgs boson[5]. However, the leptonic decays of the W boson, Z boson and top

---

[5]Also, in the case of Wh and Zh production, by the requirement to match the colour and flavour of the incoming quark and antiquark.
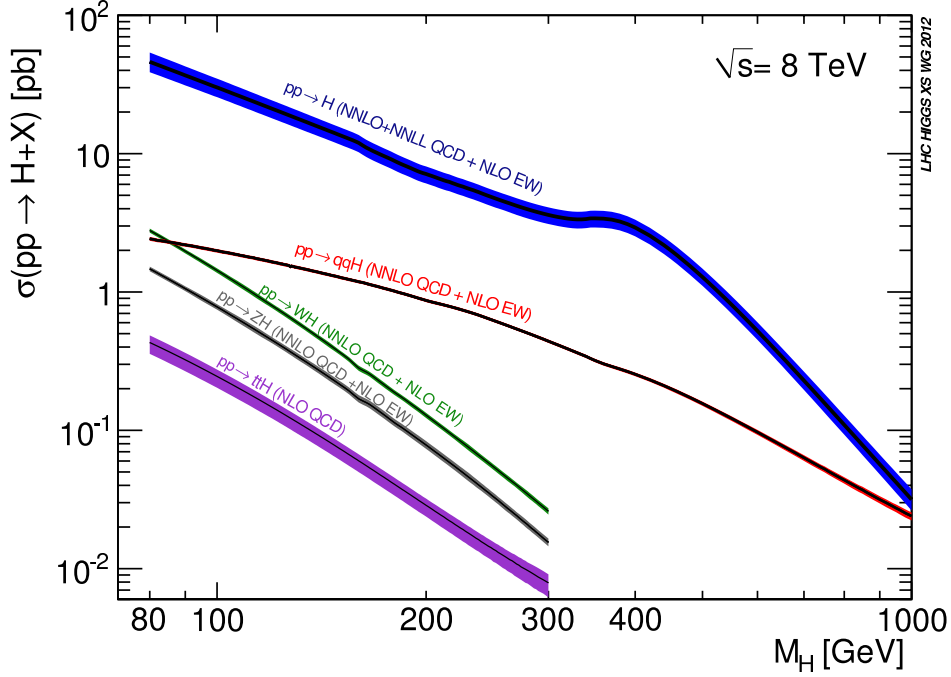
Figure 4: Cross-section for Standard Model Higgs boson production in pp collisions at $\sqrt{s} = 8$ TeV, as a function of the boson's mass.

quark can provide very powerful background rejection, and the only way to access channels such as $h \to b\bar{b}$.

In reality, experimentalists studying the Higgs boson need to take full advantage of all of the characteristics of the available production and decay modes to produce a visible signal over the various sources of background. For example, $h \to \gamma\gamma$ candidate events are separated into categories depending on whether or not the two jets characteristic of VBF are present. Figure 5 shows an example of such a VBF candidate event. When all factors are considered, it turns out that the most powerful channels, in approximate order of sensitivity, are the following (with $\ell = e, \mu$):

$\gamma\gamma$ **channel:** $h \to \gamma\gamma$;

4ℓ **channel:** $h \to 4\ell$ (i.e. $h \to ZZ^{(*)} \to \ell^+\ell^-\ell^+\ell^-$);

WW **channel:** $h \to W^\pm W^{\mp(*)} \to \ell^+\nu\ell^-\bar{\nu}$;

$\tau\tau$ **channel:** $h \to \tau^+\tau^-$;

$b\bar{b}$ **channel:** $h \to b\bar{b}$ (Wh and Zh associated production only).

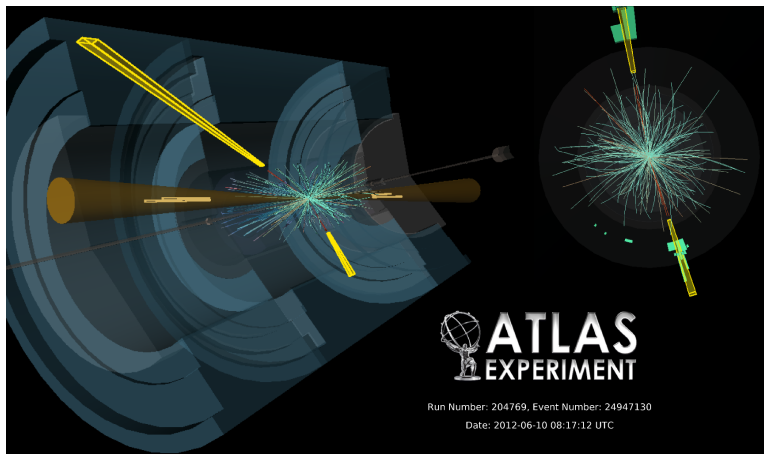For brevity, I will be referring to the channels predominantly by their short names in what follows.

Figure 5: Event display of a $h \to \gamma\gamma$ candidate event produced via VBF in ATLAS. Two reconstructed photons (yellow) form the Higgs boson candidate, while the dark brown cones indicate the two "forward" jets that help tag VBF production (see Figure 3 (c)).

3 Discovery of the Higgs boson

The two most sensitive Higgs discovery channels share an important feature: all of the final state particles (photons and charged leptons) can be fully reconstructed with high precision. The measured directions and momenta of these particles (see last tutorial) can therefore be used to construct the complete Higgs boson four-vector. The invariant mass of this four-vector should correspond to m_h, within the precision allowed by the detector's resolution. Thus, a histogram of the reconstructed Higgs boson candidate mass should display a sharp peak, while most background processes have a rate that varies relatively slowly with mass.

This is shown for the $\gamma\gamma$ and 4ℓ channels in Figure 6. In the diphoton case, the level of background is large, and comes from a mixture of genuine photons radiated from quarks and jets that are wrongly identified as photons. This leads to a smoothly varying background distribution in $m_{\gamma\gamma}$, above which a localised and well-defined peak containing nearly 1,000 events can be seen, centred at approximately 127 GeV. The background in the 4ℓ channel is much lower, arising mostly from irreducible $ZZ^{(*)}$ production, where both Z bosons decay leptonically. For this reason, it is still possible to see a clear peak at $m_h \sim 125$ GeV, despite the small Higgs branching ratio for this channel.

To claim a discovery, these distributions were analysed statistically; by convention the frequentist framework is used. The significance of the observed deviations are calculated by comparing the observed data to the background estimation without any Higgs boson production included (a "no-
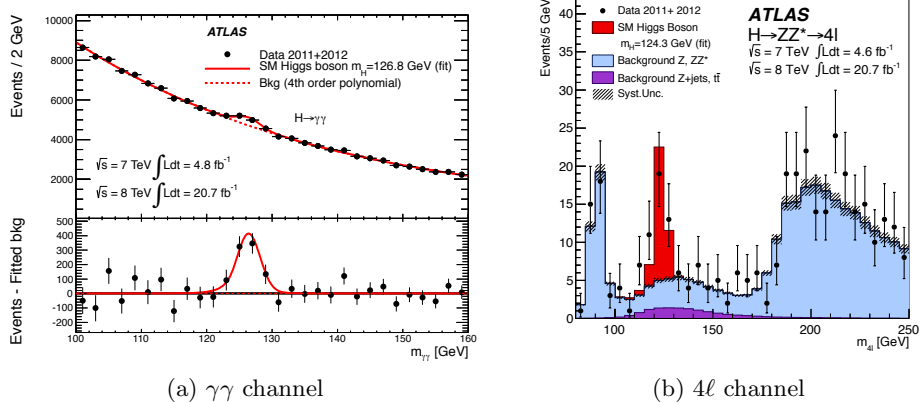
(a) $\gamma\gamma$ channel   (b) 4ℓ channel

Figure 6: Higgs candidate mass distributions in the two most sensitive channels, using data collected by the ATLAS collaboration in 2011 and 2012.

Higgs" hypothesis). The desired result is the probability (p-value) that the background, by chance, would fluctuate to a level at least as high as the observed data. If this probability is sufficiently small, a discovery can be claimed. We now explore how this is done in the simplest cases.

In the kth bin of the m_h distribution, suppose we observe n_k events, while expecting ν_k. In the absence of systematic uncertainties, i.e. assuming that ν_k is known precisely, the probability distribution for n_k is a Poissonian

$$P(n_k|\nu_k) = \frac{\nu_k^{n_k}}{n_k!} e^{-\nu_k}, \tag{2}$$

with mean and variance both equal to ν_k. In the case that ν_k is large (e.g. in Figure 6 (a)), this can be approximated by a Gaussian distribution

$$P(n_k|\nu_k) \approx \frac{1}{\sqrt{2\pi\nu_k}} e^{-\frac{(n_k-\nu_k)^2}{2\nu_k}}, \tag{3}$$

with the same mean and variance.

Exercise: Show that Equation (3) follows from Equation (2), using Stirling's approximation for the factorial, $n_k! \approx \sqrt{2\pi n_k}(n_k/e)^{n_k}$.

In this approximation, a data excess $n_k - \nu_k > 0$ can be compared to the standard deviation $\sqrt{\nu_k}$ to compute the probability of a fluctuation at least as high as n_k. In the Gaussian case, the significance (in "sigmas") is simply $(n_k - \nu_k)/\sqrt{\nu_k}$. If this ratio is greater than 3 ("3σ evidence"), the p-value is at most 0.14%. A discovery is commonly regarded as requiring a p-value of at most 2.9×10^{-7}, equivalent to a significance of 5σ. In practice, uncertainties are rarely completely Gaussian, and so the p-value is computed first, and
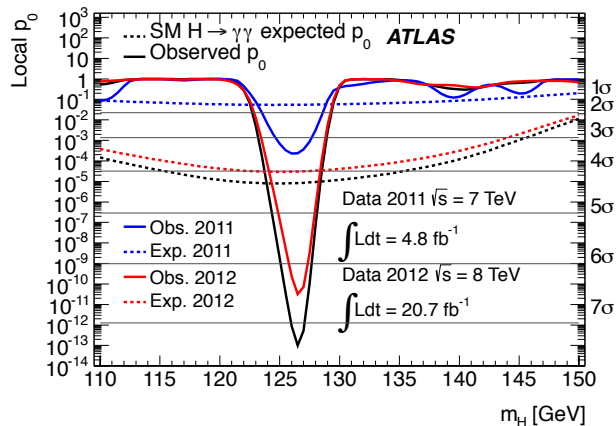
Figure 7: Scan of the *p*-value of the "no-Higgs" hypothesis and Higgs signal significance as a function of mass in the $\gamma\gamma$ channel. There is only one significant excess above the background estimation, centred at approximately 127 GeV.

the significance is calculated from that. For example, this is necessary in the 4ℓ channel, where ν_k is small.

Figure 7 shows both the *p*-value and associated significance for the $\gamma\gamma$ channel as a function of m_h. At masses far from 127 GeV, the *p*-values are close to 1, indicating compatibility with the "no-Higgs" hypothesis at that mass. However, at 127 GeV, a large deviation is seen, with a *p*-value of $\mathcal{O}(10^{-13})$, more than a 7σ excess. Similarly, the excess in the 4ℓ channel seen in Figure 6 (b) has a significance of over 6σ. Together with supporting measurements that check the quality of the collected data, these allow the discovery of a new particle to be confidently asserted.

So far, this shows that *some* kind of new phenomenon is present in the data, but it does not necessarily prove the existence of a Higgs boson. For this, many more tests are required. One relatively simple test that can be performed is to take a particular signal model (e.g. the SM Higgs boson with $m_h = 125.5$ GeV) and fit it to the observed excess. By doing this, the product of the cross-section times branching ratio ($\sigma \times \text{BR}$) for the particular channel can be measured and compared to the model prediction, averaging over the different production modes. In Figure 8, we see this measurement for the five most sensitive Higgs boson decay channels. Instead of showing $\sigma \times \text{BR}$ directly, it displays the ratio $\mu = (\sigma \times \text{BR})/(\sigma_{\text{SM}} \times \text{BR}_{\text{SM}})$, such that $\mu = 1$ corresponds to the SM. There are some variations, but overall the results are consistent with the SM. This measurement is only one of a series of measurements designed to test the hypothesis of the SM Higgs boson; we will continue to explore these in the next tutorial.
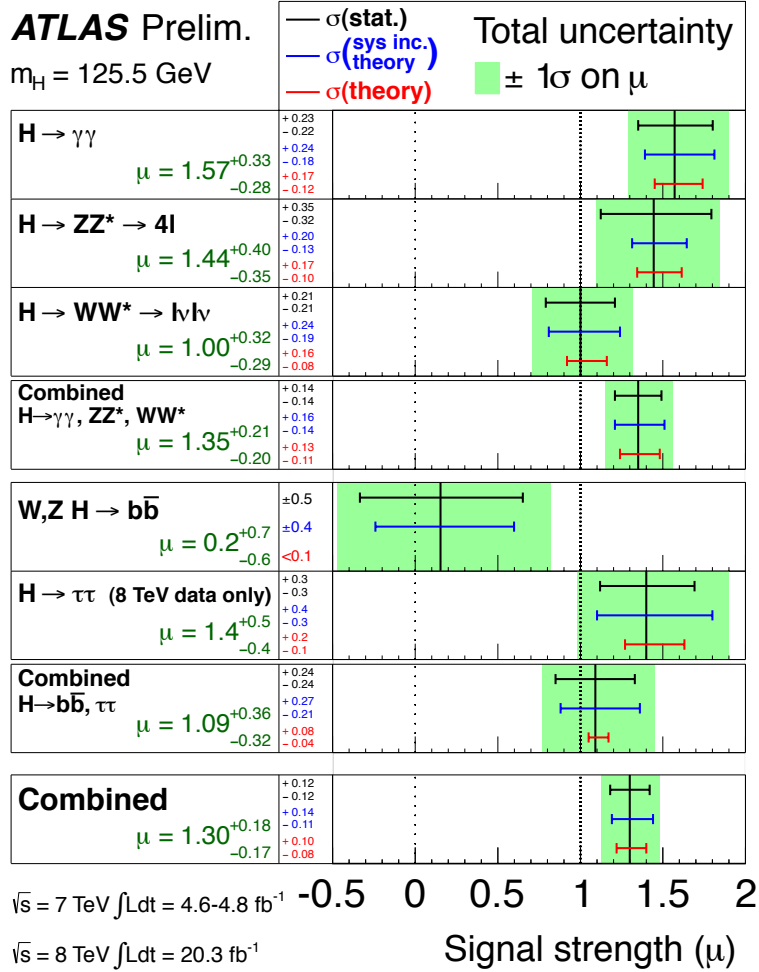
Figure 8: ATLAS summary of the observed Higgs boson signal strengths in various detection channels, relative to the SM prediction assuming $m_h = 125.5$ GeV. With all channels combined, the measured signal strength is measured to be $1.30^{+0.18}_{-0.17}$, still compatible with 1.